Published in Journal of Applied Physics 88, issue 1, 148-160, 2000
which should be used for any reference to this work

Optical absorption and light scattering in microcrystalline silicon thin films and solar cells

A. Poruba, A. Fejfar,[a] Z. Remeš, J. Špringer, M. Vaněček, and J. Kočka
Institute of Physics, Academy of Sciences of the Czech Republic, Cukrovarnická 10, CZ-162 53 Praha 6, Czech Republic
J. Meier, P. Torres, and A. Shah
Institut de Microtechnique, Université de Neuchâtel, rue Breguet 2, CH-2000 Neuchâtel, Switzerland

Optical characterization methods were applied to a series of microcrystalline silicon thin films and solar cells deposited by the very high frequency glow discharge technique. Bulk and surface light scattering effects were analyzed. A detailed theory for evaluation of the optical absorption coefficient α from transmittance, reflectance and absorptance (with the help of constant photocurrent method) measurements in a broad spectral region is presented for the case of surface and bulk light scattering. The spectral dependence of α is interpreted in terms of defect density, disorder, crystalline/amorphous fraction and material morphology. The enhanced light absorption in microcrystalline silicon films and solar cells is mainly due to a longer optical path as the result of an efficient diffuse light scattering at the textured film surface. This light scattering effect is a key characteristic of efficient thin-film-silicon solar cells.

I. INTRODUCTION

Hydrogenated microcrystalline silicon (μc-Si:H) deposited by very high frequency glow discharge (VHF-GD) methods has been introduced as a new thin film photovoltaic (PV) material[1] and leads to stable single-junction cells with over 8% efficiency and over 25 mA/cm^2 short-circuit current density.[2] The stable efficiency of the tandem microcrystalline–amorphous silicon (''micromorph'') cells, produced by VHF-plasma deposition, reached 12%.[3] Similar results were reported recently by other groups.[4,5] High efficiencies are possible thanks to a good passivation of defects by hydrogen in the μc-Si:H plasma growth process and due to an enhanced optical absorption leading to efficient sunlight absorption in just 1–4 μm thick films and solar cells.[6,7]

The important key for the success of the μc-Si:H as a PV absorbent material is its enhanced absorption compared to the monocrystalline silicon. There has been a discussion in the literature whether the observed absorption enhancement should be attributed to high internal surfaces of small crystallites, internal stress, amorphous fraction in the films or to the light scattering effects.[6,8–10] Recently we have shown that the absorption enhancement is mainly due to the light scattering[7,11] and we have suggested a procedure to identify the influence of scattering and to extract the ''true'' optical absorption coefficient $\alpha(E)$ as a function of photon energy E from the experimentally observed spectra.

This procedure is important, especially for understanding the subgap part of the optical absorption spectra related to the defect states within the energy gap. A low defect density is another prerequisite for an efficient microcrystalline solar cell. In μc-Si:H the subgap absorption is however typically very low and so we need a method which measures the absorptance down to values of 10^{-6}. Both the photothermal deflection spectroscopy (PDS) and the constant photocurrent method (CPM), well known from the field of amorphous silicon, can be used. However, both methods result in an ''apparent'' optical absorption coefficient α_{app} affected by scattering effects.

In this study we will discuss the influence of light scattering on CPM absorption spectra. CPM detects the light absorbed (either directly or after one or more scattering events) inbetween two metal electrodes used for the photocurrent measurement. Dimensions of the gap influence the contribution of the scattered light to the measured photocurrent and, thus, to the α_{app}. We will present here a procedure on how to extract from the measured α_{app} both the true optical absorption coefficient $\alpha_{\mathrm{true}}(E)$ and the contribution of light scattering.

In the case of a very weak volume scattering we have presented a theory for the evaluation of the true optical absorption coefficient $\alpha_{\mathrm{true}}(E)$.[12] In this study we present a detailed theory for the evaluation of $\alpha_{\mathrm{true}}(E)$ in scattering μc-Si:H samples in the subgap and above-gap regions from spectrophotometric measurements of transmittance $T(\lambda)$ and reflectance $R(\lambda)$ and from the absorptance $A(\lambda)$ measured by CPM. Both scattering effects, i.e., at the surface and in the bulk of the film, are included in our analysis. We verify our theory with the experimental results for different μc-Si:H films. We show how the spectral dependence of $\alpha_{\mathrm{true}}(E)$ can be interpreted in terms of defect density, disorder, crystalline/amorphous fraction and material morphology. Finally, we will discuss the correlation of μc-Si:H

[a]Author to whom correspondence should be addressed; electronic mail: fejfar@fzu.cz

properties and light trapping effects with a boost of the solar cell performance.

II. THEORY

A. Parameters used to describe light scattering in the volume and at the surface of μc-Si:H

In the following let us consider a light beam incidenting perpendicularly on a thin μc-Si:H film deposited on a thick nonabsorbing substrate with a corresponding refractive index n_s and surrounded by an ambient with a real refractive index n_a. The parameters of the film are denoted by the index f: thus, the film thickness is d_f and its complex refractive index is $N_f = n_f + ik_f$. The imaginary part of the refractive index k is related to the optical absorption coefficient α by

$$k = \frac{\lambda}{4\pi}\alpha. \tag{1}$$

For the dispersion of the μc-Si:H refractive index n_f we use a modification of the Sellmeier formula suggested by Herzberger[13]

$$n_f = n_A + \frac{n_B}{\lambda^2 - 0.028}, \tag{2}$$

where n_A and n_B are material constants which have to be determined experimentally, the vacuum wavelength λ is given in micrometers and the choice of the constant 0.028 is arbitrary and independent of the material. The advantage of Herzberger's formula is the linear relation between the refractive index and its parameters, which will be useful for fitting the interference fringes in the $R(\lambda)$ and $T(\lambda)$ spectra.

Light scattering occurs both at inhomogeneities in the volume (mostly voids) and at the surface of the μc-Si:H film. Both effects lead to the attenuation of the specular reflected and transmitted beams and to an enhancement of the absorption. The typical rms surface roughness σ, observed by atomic force microscopy (AFM), is 10–40 nm for 2 μm thin films.[11] Fourier transform analysis of the AFM data revealed a small correlation distance. The grains in the layer, typically prolonged in the direction of growth, have a diameter on the order of tens of nanometers.[14] Hence, we can use the scalar scattering theory for random rough surfaces with a small correlation distance.[15]

The losses from the specular light beam by scattering at the rough interface between media 1 and 2 are described within the scalar theory by the scattering factors s.[15] Thus, in comparison with a smooth interface, the Fresnel coefficient r_{12} for the amplitude of the beam reflected from the rough surface back to the medium 1 is reduced by a factor

$$s_{12}^{r} = \exp\left[-\frac{1}{2}\left(\frac{4\pi n_1 \sigma}{\lambda}\right)^2\right] \tag{3}$$

and the Fresnel coefficient t_{12} for the amplitude of the beam transmitted through the rough interface to medium 2 is reduced by a factor

$$s_{12}^{t} = \exp\left[-\frac{1}{2}\left(\frac{2\pi(n_1 - n_2)\sigma}{\lambda}\right)^2\right], \tag{4}$$

where σ is the rms surface roughness of the boundary interface, n_1 and n_2 are the refractive indices of the corresponding media, and λ is the light wavelength in vacuum (see also Appendix A). Formulas (3) and (4) assume: (i) $\sigma \ll \lambda$, (ii) small correlation length of the surface roughness and (iii) normal incidence of the light. In the case of an oblique incidence the surface roughness σ has to be reduced by the factor $\sin(\gamma)$, where γ is the angle between the surface and the direction of the incoming light beam.

On the other hand, the attenuation of the specular light beam by an isotropic volume scattering may be simply described by the volume scattering coefficient α_{sc}.[16] Therefore, the attenuation of the specular beam in the film is given by the coefficient α_f

$$\alpha_f = \alpha_{true} + \alpha_{sc}, \tag{5}$$

where α_{true} is the true optical absorption coefficient in the film.

The description of the scattering by s factors and by α_{sc} is the simplest description of the otherwise complex phenomenon and expresses the level of approximations we use.

B. Specular reflectance and transmittance of scattering samples and determination of the optical constants

The description of the specular reflectance and transmittance of a μc-Si:H layer on a thick glass substrate needs to take into account both μc-Si:H interfaces, multiple reflections within the layer as well as the influence of the back substrate–ambient interface. The resulting formulas for the spectra of reflectance from the film side $R_f(\lambda)$ or from the side of the substrate (typically glass) $R_g(\lambda)$ and the transmittance $T(\lambda)$ as a function of the sample parameters n_f, α_f, d_f, σ, n_a, n_s are complicated functions given in full detail in Appendix A. As an example, the reflectance and transmittance calculated for a 1 μm thick μc-Si:H layer on a thick glass substrate are shown in Fig. 1. The results plotted by full lines correspond to the sample with a smooth top surface and those plotted by the dashed lines for a surface with the rms roughness $\sigma = 30$ nm. One can observe that the rough surface leads to a decrease of both reflectance and transmittance and also to a partial smoothing of the interference fringes.

Figure 1 shows the T and R results of modeling for known film parameters, but in the experiment, we need to solve the inverse problem, i.e., the determination of the sample parameters n_f, α_f, d_f and σ from the measured $R_f(\lambda)$, $R_g(\lambda)$ and $T(\lambda)$. For that purpose we divide the spectra into three regions:

(i) a region of strong (complete) absorption ($T_f = T_g \sim 0$) where the surface roughness and refractive index $n_f(\lambda)$ of the film can be estimated;

(ii) a region with negligible absorption ($\alpha_f \sim 0$) where the film thickness and refractive index $n_f(\lambda)$ can be estimated; and

(iii) a region of medium and high absorption ($T_f = T_g > 0$ where the $\alpha_f d_f$ product is in the range 0.05–5) where the absorption coefficient $\alpha_f(\lambda)$ can be determined.

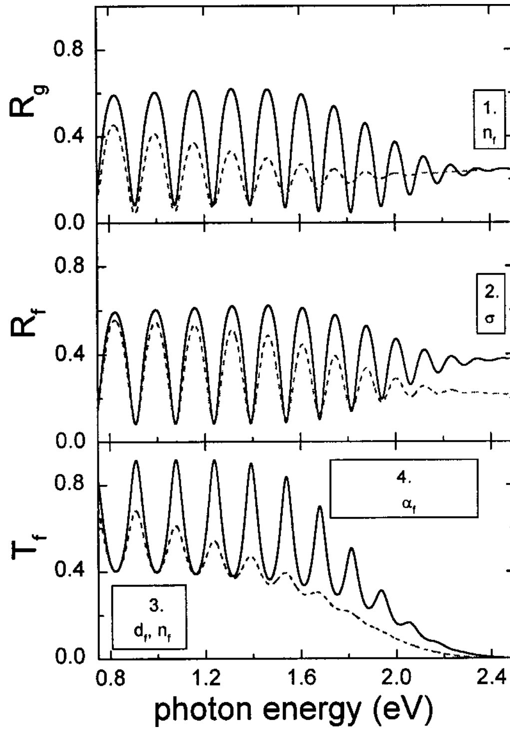

FIG. 1. Calculated spectra of reflectance R_g, R_f and transmittance T_f of a μc-Si:H layer on a glass substrate according to the formulas given in Appendix A for a smooth surface (solid lines) and for a layer with a rms roughness of σ=30 nm (dashed lines). The subscripts f and g indicate that we consider light incidence on the sample from the side of the film, respectively from the glass substrate. Note that $T_f = T_g$. The refractive index of the μc-Si:H layer was approximated by $n_f = 3.3 + 0.2/(\lambda^2 - 0.028)$ and the absorption coefficient by $a_f = 15\,000^*(E-1.1)^4(\mathrm{cm}^{-1})$. The boxes mark the spectral regions from which the optical parameters of the sample are obtained: (1) refractive index of the film n_f is obtained from the value of R_g in the region of strong absorption; (2) rms roughness σ is obtained from the difference of the R_f expected for the smooth film and actually observed in the region of the strong film absorption; (3) the film thickness d_f and refractive index dependence $n_f(\lambda)$ are found from the region of negligible absorption; (4) the absorption coefficient of the film $a_f(\lambda)$ is obtained from the region of medium absorption.

These spectral regions are marked in Fig. 1 together with the parameters that can be obtained from them. Let us consider these regions in more detail as methodical steps (1–3) for the evaluation.

1. Determination of the surface roughness and real part of the refractive index in the high absorption region

The real part n_f of the film refractive index and the surface roughness σ can be found from the measurements of the sample reflectance R_f and R_g in the region of complete absorption where the interference effects are suppressed. Thus, we may neglect the multiple reflections in the film and consider only the first-order terms for reflected light in Eq. (A5) of Appendix A. The formula (A11) for the reflectance of the sample R_{sfa} from the substrate side is simplified to

$$R_{\mathrm{sfa}} = R_{\mathrm{sf}} = \left| \frac{N_f - n_s}{N_f + n_s} \right|^2. \tag{6}$$

Neglecting the imaginary part k_f of the film refractive index $N_f = n_f + ik_f$ (in this spectral range $k_f \leqslant 0.1 \ll n_f \sim 3.8$) we can express the film refractive index n_f as

$$n_f = n_s \frac{1 + R_{\mathrm{sf}}}{1 - R_{\mathrm{sf}}}, \tag{7}$$

where R_{sf} can be calculated from the experimentally observed reflectance R_g using Eq. (A14)

$$R_{\mathrm{sf}} \doteq R_{\mathrm{sfa}} = \frac{R_g - R_{\mathrm{as}}}{T_{\mathrm{as}}^2 + R_{\mathrm{as}} \cdot (R_g - R_{\mathrm{as}})}. \tag{8}$$

Here R_{as} is the reflectance and T_{as} the transmittance of the substrate–ambient interface which can be calculated from the known refractive indexes of the substrate and the ambient.

While the reflectance R_g measured from the substrate side is not influenced by the rough free film surface, the reflectance measured from the side of the film R_f will be reduced by scattering. With the value of n_f determined by Eq. (7) we can now calculate the surface roughness from the measured R_f at the same wavelength:

$$\sigma = \frac{\lambda}{4\pi n_a} \ln \sqrt{R_f \cdot \left(\frac{n_f + n_a}{n_f - n_a} \right)^2}. \tag{9}$$

An estimated rms surface roughness σ by Eq. (9) simplifies further calculations.

2. Determination of the sample thickness and refractive index from the interference fringes in the low absorption spectral region

The thickness of the film d_f and the spectral dependence of n_f (i.e., the parameters n_A and n_B [Eq. (2)] of Herzberger's formula) can be calculated from the interference fringes in the reflectance and transmittance spectra using a multiparameter fitting procedure.[17] We need to fit three parameters and in order to avoid any divergence problem we divide the fitting procedure into two parts.

First we fit the spectral dependence of the refractive index. The formulas for reflectance R_g or R_f of the sample, Eq. (A14), can be rewritten into the form

$$y(\lambda) = \frac{1}{1-R} = a(\lambda) + b(\lambda) \cdot \cos(\varphi), \tag{10}$$

where $a(\lambda)$ and $b(\lambda)$ are functions of the index of refraction: n_f, n_s, and n_a and $\varphi = 4\pi n_f d_f/\lambda$. A useful expression can be obtained by considering the envelopes around the maxima $y_{\mathrm{max}}(\lambda) = a(\lambda) + b(\lambda)$ and minima $y_{\mathrm{min}}(\lambda) = a(\lambda) - b(\lambda)$ of the $y(\lambda)$ spectrum. These envelopes are considered to be continuous functions of λ. We obtain the functions $a(\lambda)$ and $b(\lambda)$ by a spline interpolation of the experimentally observed y_{max} and y_{min}. Once $a(\lambda)$ and $b(\lambda)$ are known, we can calculate $\cos(\varphi) = (y(\lambda)) - a(\lambda))/b(\lambda)$. Now using Herzberger's dispersion formula, i.e., Eq. (2), we can express $\cos(\varphi)$ as

$$\cos(\varphi)=\cos\left(\frac{4\pi n_f d_f}{\lambda}\right)$$
$$=\cos\left[\frac{4\pi E}{1.2389}\left(p_A+\frac{p_B}{(1.2389/E)^2-0.028}\right)\right], \quad (11)$$

where $E=1.2389/\lambda$ is the photon energy in eV and p_A and p_B are parameters related to n_A and n_B by the expressions $p_A=n_A d_f$ and $p_B=n_B d_f$ (where d_f and λ are expressed in micrometers). Parameters p_A and p_B are found by a nonlinear least-squares fitting of the spectral dependence of $\cos(\varphi)$ obtained from measured T/R using Eq. (11).

Using the obtained p_A and p_B we can calculate $\cos(\varphi)$ at each λ in the formulas for the reflectance and transmittance of the film [Eqs. (A10)–(A11)]. A nonlinear least-squares fitting routine used to fit the transmittance or reflectance data in the transparent region then requires only the free parameter d_f, which is easy to obtain.

3. Imaginary part of the index of refraction from the region of medium absorption

When the spectral dependence of $n_f(\lambda)$ and the thickness of the film d_f are known we can find the spectrum of $a_f(E)$. In the spectral region where the film absorption coefficient is high enough and the interferences in the film are absent the absorption coefficient can be calculated directly from the transmittance using Eq. (A12) reduced to the form

$$T'=\frac{T_{\rm af}T_{\rm fs}T_{\rm sa}\exp(-a_f d_f)}{1-R_{\rm sf}R_{\rm sa}}, \quad (12)$$

where $T_{\rm af}$, $T_{\rm fs}$, $T_{\rm sa}$ can be calculated using the known values for σ, d_f, n_a, n_s and n_f (n_f is extrapolated from the Herzberger's formula using n_A and n_B determined in the transparent region).

The approach based only on the transmittance fails in the region of week absorptance, because the influence of the interference effects on the transmittance spectra drowns the influence of the absorption. The inspection of Eqs. (A10)–(A12) shows that the function $(1-R_g)/T$ is almost free of interference fringes[18] and is, thus, suitable to solve $\alpha_f(E)$. This approach makes it possible to calculate values of α_f in the spectral region, where $\alpha_f d_f \geqslant 0.05$.

C. Measurement of the absorptance in samples with the bulk or the surface scattering by CPM

CPM uses the photocurrent proportional to the amount of light absorbed in the film. For nonscattering samples on nonabsorbing substrates the photocurrent is simply proportional to the absorptance defined as

$$A=1-R-T, \quad (13)$$

where R and T are the reflectance and the transmittance. More care is required for the analysis of scattering samples. Here, a large part of the light scattered in the silicon film (with relatively high refractive index) will remain trapped in the film by total internal reflections and, thus, scattering will actually lead to a much more efficient photogeneration of the carriers mainly in the low absorption range. Finally, it is important to realize that due to the short diffusion lengths of the carriers only the light absorbed between the electrodes will contribute to the photocurrent. The geometry of the coplanar electrodes with width W and distance D used for CPM measurements is shown in Fig. 2.

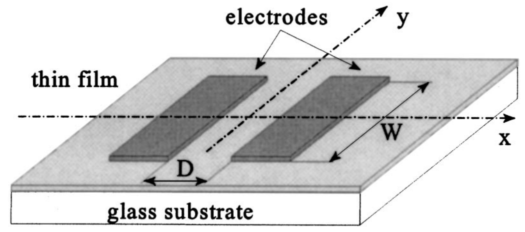

FIG. 2. Electrode configuration for the measurement of the photocurrent in the constant photocurrent method (CPM).

The details of the CPM method and evaluation are described elsewhere.[19] The most simple standard interpretation of the measured CPM spectra[20] uses the Beer's law expression for the absorptance of the film

$$A=(1-R)[1-\exp(-\alpha d)]. \quad (14)$$

For small values of α this leads to $A \doteq (1-R)\alpha d$. Furthermore, changes in the reflectance R as a function of photon energy E can be neglected, when compared with changes in α over several orders of magnitude. A similar assumption has been made in PDS.[21] Keeping the photocurrent constant by changing the intensity of the illumination leads to a simple evaluation of the $\alpha(E)$ spectrum, which is proportional to the inverse of the photon flux. In the following we shall denote the result of this procedure as the apparent absorption coefficient $\alpha_{\rm app}$. More precise expressions for the absorptance, which would include the effect of the multiple reflections, can be used (see Appendix A) but the arguments of Sec. II C 1 remain valid.

1. Model of multiple bulk scattering

If we use the simple approach (Beer's law) for bulk scattering in the films, the attenuation of the specular beam will be given by Eq. (14) with absorption coefficient $\alpha_f=\alpha_{\rm true}+\alpha_{\rm sc}$ [Eq. (5)]. Hence, neglecting the spectral dependence of reflection, the part of light directly absorbed will be

$$A_{\rm dir}\approx\frac{\alpha_{\rm true}}{\alpha_f}\cdot[1-\exp(-\alpha_f d_f)] \quad (15)$$

and the part of light scattered in the volume of the film will be

$$A_{\rm sc}\approx\frac{\alpha_{\rm sc}}{\alpha_f}\cdot[1-\exp(-\alpha_f d_f)]. \quad (16)$$

Correspondingly the photocurrent will be composed of two components

$$I_{\rm ph}=I_{\rm dir}+I_{\rm sc}, \quad (17)$$

where $I_{\rm dir}$ is proportional to $A_{\rm dir}$ and represents the photocurrent excited by photons absorbed from the specular beam, i.e., without any scattering

$$I_{\rm dir}\approx N_{\rm photons}A_{\rm dir}\approx N_{\rm photons}\cdot\frac{\alpha_{\rm true}}{\alpha_f}\cdot[1-\exp(-\alpha_f d_f)], \tag{18}$$

where $N_{\rm photons}$ is the incident photon flux.

The component $I_{\rm sc}$ represents the contribution of photons absorbed after one or more scattering events. This component is important mainly at the spectral region with low optical absorption coefficient $\alpha_{\rm true}$. It will be proportional to the number of photons scattered from the specular beam $A_{\rm sc}$ defined by Eq. (16), however we need also to consider the probability that the scattered photon will be absorbed in the space between the electrodes and thus will contribute to the observed photocurrent.

First, let us define a very important parameter for the light trapping scheme, the critical angle θ for total reflections. θ defines the escape cone and can be calculated from the total internal reflection condition $\sin(\theta)=n/n_f$, where n is the index of the outer medium. For the refractive index of 3.5 (for μc-Si:H films in the near IR region) this gives $\theta\doteq16.6°$ for the film–air interface and $\theta\doteq25.4°$ for the film–glass interface. If the photon from the specular beam is scattered in the direction outside of the escape cone it will be confined within the film by total internal reflections and will remain trapped until it is either absorbed or scattered again. If the photon is scattered within the escape cone it will probably escape from the film after a few internal reflections. A numerical simulation shows that the contribution of such photons to the photocurrent is negligible. Assuming isotropic scattering we can write the probability $P_{\rm tr}$ that the photon is scattered outside the escape cone as

$$P_{\rm tr}=\cos\theta. \tag{19}$$

When the scattered photon is trapped by the waveguiding it must finally be absorbed or scattered again. The probability that this photon will be scattered is determined by the value of the mean free path between two scattering events. The mean free path is given as a reciprocal value of the scattering coefficient $\alpha_{\rm sc}$ (typical values in microcrystalline silicon for $\alpha_{\rm sc}$ are $\lesssim 50\times E^4\ {\rm cm}^{-1}$, where E is the photon energy in eV[7]). The probability that the waveguided photon is absorbed within its mean free path is $1-\exp(-\alpha_{\rm true}/\alpha_{\rm sc})$. If the photon is not absorbed during the mean free path $1/\alpha_{\rm sc}$ it is scattered again and the same kind of considerations are valid. The photocurrent excited by scattered photons can then be calculated by the sum of these contributions, leading to a geometrical series (see Appendix B for details).

However, the absorbed photon will contribute to the photocurrent with probability P_{WD} only if it is absorbed within the area between electrodes (see Fig. 2). Finally the contribution of the scattered light to the photocurrent observed by CPM will be proportional to the product (with the same constant as the $I_{\rm dir}$ component)

$$I_{\rm sc}\sim N_{\rm photons}A_{\rm sc}P_{\rm tr}P_{WD}, \tag{20}$$

which leads to the expression (for details see Appendix C)

$$I_{\rm sc}\approx N_{\rm photons}\frac{\alpha_{\rm sc}}{\alpha_f}\exp(-\alpha_f d_f)\cdot\cos\theta \cdot\left[1-\exp\left(-\frac{\alpha_{\rm true}}{\alpha_{\rm sc}}\right)\right]\frac{\left[\cos\theta\cdot\exp\left(-\frac{\alpha_{\rm true}}{\alpha_{\rm sc}}\right)\right]^{N_{\rm bulk}}-1}{\cos\theta\cdot\exp\left(-\frac{\alpha_{\rm true}}{\alpha_{\rm sc}}\right)-1}, \tag{21}$$

where $N_{\rm bulk}$ is the number of the scattering events between the electrodes. For the determination of this parameter we use the solution of the classical probability task—a random walk:

$$N_{\rm bulk}=[\alpha_{\rm sc}\cdot X(W,D)]^2, \tag{22}$$

where $X(W,D)$ is the function of electrode dimensions which gives a value approximately equal to the distance between the electrodes when the ratio of the length of electrodes and the interelectrode spacing is close to the value of 6.6—for details see Appendix C.

If the standard CPM evaluation procedure will be applied to the measured spectrum, we will obtain an apparent optical absorption coefficient $\alpha_{\rm app}$ for which the following equation is valid:

$$1-\exp(-\alpha_{\rm app}\cdot d_f) =\frac{1}{\alpha_f}\cdot[1-\exp(-\alpha_f\cdot d_f)]\cdot\left[\alpha_{\rm true}+\alpha_{\rm sc}\cdot\cos\theta \cdot\left[1-\exp\left(-\frac{\alpha_{\rm true}}{\alpha_{\rm sc}}\right)\right] \cdot\frac{\left[\cos\theta\cdot\exp\left(-\frac{\alpha_{\rm true}}{\alpha_{\rm sc}}\right)\right]^{N_{\rm bulk}}-1}{\cos\theta\cdot\exp\left(-\frac{\alpha_{\rm true}}{\alpha_{\rm sc}}\right)-1}\right]. \tag{23}$$

This equation shows how the CPM measured $\alpha_{\rm app}$ depends on the electrode geometry, i.e., the interelectrode spacing D and the electrode length W (see Fig. 2), and on the parameters $\alpha_{\rm true}$, $\alpha_{\rm sc}$ and n_f (n_f influences the value of the critical angle for the total reflection).

The combination of Eqs. (23) and (5) enables the modeling of the apparent optical absorption coefficient $\alpha_{\rm app}$ of the film with the known parameters $\alpha_{\rm true}$, $\alpha_{\rm sc}$, θ, W and D. Note that although the film thickness appears also in Eq. (23), this parameter does not influence the result of modeling. The inverse problem, i.e., the evaluation of the spectral dependence of the absorption coefficient $\alpha_{\rm true}$ and the scattering coefficient $\alpha_{\rm sc}$ cannot be solved analytically and numerical methods have to be used. First we roughly estimate the scattering coefficient $\alpha_{\rm sc}$ from a comparison of several CPM measurements (for different interelectrode spacing) with the model output data of the same coplanar geometries. In agreement with Ref. 22 we suppose the spectral dependence of the scattering coefficient. For the value of the scat-

tering coefficient α_{sc} (at photon energy $E=1$ eV) up to 50 cm^{-1} we suppose the Rayleigh type of scattering, i.e., a dependence $\approx E^4$. The estimated scattering coefficient (and its spectral dependence) together with the smoothed CPM data enter the iterative procedure of evaluation of the true absorption coefficient.

2. Model of surface scattering

Most of the high quality microcrystalline silicon films do not exhibit a mirrorlike free surface. These layers with a ''milky'' appearance have a typical rms surface roughness of 15–35 nm, which leads to the surface scattering. We present here the theory for surface scattering derived by the help of s factors for the case of light entering from the film side. For these calculations we introduce new factors S_t, S_r and S_{r0} which decrease the intensity of the specularly transmitted or reflected wave. These factors are defined as[15]

$$S_t=s_{\mathrm{af}}^2=s_{\mathrm{fa}}^2=\exp\left[-\left(\frac{2\pi(n_f-n_a)\sigma}{\lambda}\right)^2\right], \tag{24}$$

$$S_{r0}=s_{\mathrm{ff}}^2=\exp\left[-\left(\frac{4\pi n_f\sigma}{\lambda}\right)^2\right], \tag{25}$$

$$S_r=\exp\left[-\left(\frac{4\pi n_f\sigma\cos\varphi}{\lambda}\right)^2\right], \tag{26}$$

where S_{r0} corresponds to the perpendicular internal reflection and S_r to the oblique incidence with the angle of incidence φ (with respect to the surface normal). Since we calculate an average amount of the scattered light for all angles, we use the following empirical formula (taking into account a change of the critical angle of total reflection with a change of the index of refraction):

$$S_r=\exp\left[-\left(\frac{4\pi n_f\sigma\cos(\pi/n_f)}{\lambda}\right)^2\right]. \tag{27}$$

For CPM modeling in the case of rough samples, we start again with Eq. (17) for the photocurrent passing through the sample (consisting of I_{dir} and I_{sc}). I_{dir} (photocurrent after photon absorption without any scattering event in thin film of thickness d_f) is given by

$$I_{\mathrm{dir}}\approx N_{\mathrm{photons}}\cdot S_t\cdot[1-\exp(-\alpha_{\mathrm{true}}\cdot d_f)]. \tag{28}$$

The component I_{sc} represents the contribution of photons absorbed after one or more scattering events. This component is important not only in the low absorption range (as in the case of bulk scattering) but also at the spectral region with medium (and high) optical absorption coefficient α_{true}. It is proportional to the number of photons scattered from the specular beam by the rough interface and absorbed in the region of electric field.

The number of photons scattered during the passage through the rough ambient–film interface is proportional to $(1-S_t)$. Nevertheless, we also consider here the contribution of photons scattered by more complicated ways after specular transmission through the first interface, the penetration through the film, then the reflection at the second (smooth) film–substrate interface, followed again by the penetration through the film, and finally the diffusive reflection at the first interface. The total amount of the scattered light is then in relation to the probability P_0

$$P_0=(1-S_t)+S_t\cdot R_{\mathrm{fs}}\cdot\exp(-2\alpha_{\mathrm{true}}d_f)R_{\mathrm{fa}}(1-S_{r0}). \tag{29}$$

The parameters R_{fs} and R_{fa} are the reflection coefficients at the interface film–substrate and film–air, respectively. The second part of the right hand side of Eq. (29) is usually smaller but not negligible in comparison with the first one, because $(1-S_{r0})$ can be an order of magnitude higher than $(1-S_t)$.

Waveguiding properties of the material are determined again by the critical angle θ for the total reflection which defines the escape cone. The probability P_{esc} that a photon will be scattered within the escape cone is given for the ideal Lambertian (cosine) distribution as

$$P_{\mathrm{esc}}=\left(\frac{n_s}{n_f}\right)^2. \tag{30}$$

For surface scattering the smallest distance between two scattering events is given by twofold thickness of the film (for the photons scattered in the specular direction). On the other hand, the longest distance is infinite for the light scattered parallel to the film plane. The total Lambertian angle distribution (φ from 0 to $\pi/2$) is given by $\cos(\varphi)\sin(\varphi)$ product with a maximum at the angle $\varphi=\pi/4$. The multiplication factor Y for the average increase of the optical path of the scattered light, compared to the sample thickness, can be calculated from the angular distribution as

$$Y=2\cdot\frac{\int_\theta^{\pi/2}\sin\varphi d\varphi}{\int_\theta^{\pi/2}\sin\varphi\cos\varphi d\varphi}, \tag{31}$$

where the factor 2 means twofold path because of the total internal reflection at the film–substrate smooth interface. [The parameter Y varies for μc-Si:H with the index of refraction (wavelength) from about 4.2 to 4.6.] Hence, for very rough samples, the $Y\cdot d_f$ product denotes something like the mean free path. For microcrystalline silicon films with rms surface roughness typically varying from 15 to 35 nm, the probability of a photon being absorbed during this distance $(Y\cdot d_f)$ is equal to $[1-\exp(-Y\alpha_{\mathrm{true}}d_f)]$ and the probability of being scattered at this rough interface is given by $(1-S_r)$. If the photon is neither absorbed nor scattered or if the photon is not absorbed but is scattered outside the escape cone, then the same kind of considerations have to be applied again. The calculation of the photocurrent I_{sc} leads to the solution of a geometrical series and is given by

$$I_{\mathrm{sc}}\approx P_0A_1+P_0P_1A_2\cdot\frac{P_2^{N_{\mathrm{surf}}}-1}{P_2-1}, \tag{32}$$

where

$$A_1=(1-P_{\mathrm{esc}})\cdot[1-\exp(-Y\alpha_{\mathrm{true}}d_f)]+P_{\mathrm{esc}}\cdot[1-\exp(-1.05\alpha_{\mathrm{true}}d_f)], \tag{33}$$

where A_1 represents the relative amount of scattered light absorbed between the first and the second scattering event

and the factor 1.05 is the average increase of the optical path of the scattered light within the escape cone (for the μc-Si:H film/glass interface).

$$P_1=(1-P_{\text{esc}})\cdot\exp(-Y\alpha_{\text{true}}d_f) \tag{34}$$

is the relative reduction of the light intensity between the first and the second scattering event

$$\begin{aligned}A_2=&[(1-P_{\text{esc}})\cdot(1-S_r)+S_r]\cdot[1-\exp(-Y\alpha_{\text{true}}d_f)]\\&+P_{\text{esc}}\cdot[1-\exp(-1.05\alpha_{\text{true}}d_f)]\\&\cdot[1+R_{\text{fs}}\cdot\exp(-1.05\alpha_{\text{true}}d_f)]\end{aligned} \tag{35}$$

is the relative amount of the scattered light absorbed between the next two scattering events (second and third, third and fourth, ...) and

$$P_2=[(1-P_{\text{esc}})\cdot(1-S_r)+S_r]\cdot\exp(-Y\alpha_{\text{true}}d_f)] \tag{36}$$

is again the relative light intensity reduction between the next two scattering events.

The total number of scattering events inside the region of the electric field N_{surf} in the case of surface scattering can be calculated by weighting the probability $(1-S_r)$ of photons to be scattered at a distance Yd_f and probability S_r of photons to be specularly reflected

$$N_{\text{surf}}=\left(\frac{X(W,D)}{Yd_f}\right)^2\cdot(1-S_r)+\left(\frac{X(W,D)}{Yd_f}\right)\cdot S_r, \tag{37}$$

where $X(W,D)$ is the interelectrode spacing function (see Appendix C).

For the modeling we take into account that a part of the light escaping to the (nonabsorbing) glass substrate (with index of refraction $n_s\approx 1.5$ and substrate thickness d_s) can return to the area of the electric field between the electrodes. This consideration leads to the modification of the relative amount of the photons within the escape cone and, thus, the probability P_{esc}, which will vary not only with the index of refraction of the film and substrate (n_f and n_s), but also with the substrate thickness d_s and the interelectrode function $X(W,D)$. P_{esc} is given by

$$P_{\text{esc}}=\left(\frac{n_{s\text{ef}}}{n_f}\right)^2, \tag{38}$$

where $n_{s\text{ef}}$ (varying from n_a to n_s) represents the effective index of refraction of the substrate which can be calculated (for the cosine distribution of the scattered light) as

$$n_{s\text{ef}}=\left(1+n_s^2-\left\{n_s\cdot\sin\left[\arctan\left(\frac{X(W,D)}{2d_s}\right)\right]\right\}^2\right)^{0.5}. \tag{39}$$

Now, we can write for the apparent optical absorption coefficient as measured by CPM

$$\begin{aligned}1-\exp(-\alpha_{\text{app}}\cdot d_f)=&S_t[1-\exp(-\alpha_{\text{true}}\cdot d_f)]\\&+P_0\left(A_1+P_1A_2\frac{P_2^{N_{\text{surf}}}-1}{P_2-1}\right).\end{aligned} \tag{40}$$

Similarly as in the case of the multiple bulk scattering, this equation can be used for modeling of the apparent optical absorption coefficient α_{app} with the help of the known parameters $\alpha_{\text{true}}(E)$, σ, d, d_s, $n(E)$, W and D. The evaluation of $\alpha_{\text{true}}(E)$ from the CPM measurement is done numerically on the basis of the known rms surface roughness σ, determined optically.

III. EXPERIMENT

Microcrystalline silicon layers and solar cells were deposited by the VHF-GD method using high dilution of silane in hydrogen, with and without a purifier.[2,3,23] Layers were deposited on AF45 glass, under conditions similar to the corresponding cells. The typical film thickness was around 2 μm. With respect to the deposition conditions the layers result in either a smooth, mirrorlike or a rough, hazy appearance. Some rough (textured) layers were afterwards chemomechanically polished to a mirrorlike surface to exclude the influence of the rough surface on the measurement of optical properties. This is a delicate procedure, frequently ending with the layer peeling off from the substrate.

The typical rms surface roughness of (220) textured microcrystalline Si layers is below 40 nm for about 2 μm thick films, as directly observed by the AFM. The grains in the layer, prolonged in the direction of growth, have an effective diameter of 10–30 nm, as seen by transmission electron microscopy (TEM).[14]

A computer-controlled single-beam spectrometer was used for the transmittance/reflectance measurements in the 0.6–3 eV spectral region. The diameter of the light beam was limited to 1 mm in order to suppress the influence of possible variations of the layer thickness on the modulation depth of the interference fringes. The detector (or the integrated sphere with a detector) is placed far behind the sample; hence, just the specular reflectance and transmittance are measured.

The CPM setup described elsewhere[19] was used to measure the absorptance of the films both in the standard and absolute CPM mode. On top of the layers coplanar Al or Cr/Ag electrodes were evaporated with the interelectrode spacing D varying from 30 μm to 3 mm and electrode width W between 2 and 8 mm (Fig. 2). The contribution of the scattered light to the CPM signal is changed by this geometrical setup of the electrodes.[7]

IV. RESULTS

The spectral dependence of the specular transmittance and reflectance of a typical layer before and after the polishing is shown in Fig. 3. Just a part of the reflectance data is displayed here. In the case of textured surfaces, the modulation depth of the interference fringes is reduced due to light scattering. The ''scalar scattering theory,'' which considers just the phase modulation of the incident and outgoing light by the height variations along the surface, has been used to interpret the data and to evaluate the root mean square (rms) surface roughness σ by the procedure described in Sec. II A.[24]

Calculated values of the optical absorption coefficient α for the sample from Fig. 3 are shown in Fig. 4 and compared with the absorption coefficient of crystalline silicon.[25] Perfect agreement of the $\alpha_{\text{true}}(E)$ evaluated from the T and R measurements on the polished (σ=0) and on the ''as grown''

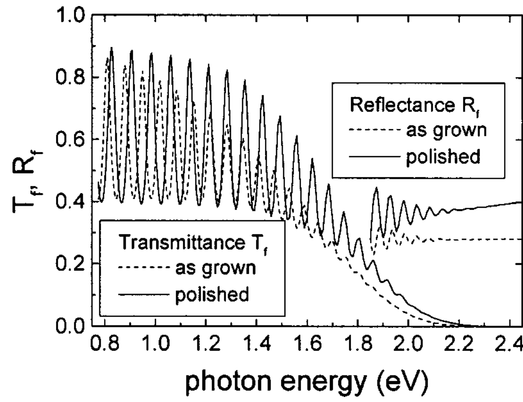

FIG. 3. Transmittance and reflectance spectra of a μc-Si:H sample, deposited with 5% dilution of silane in the total gas flow at a VHF deposition power of 19 W. Dashed lines show the results before polishing (textured surface with rms roughness σ=24 nm) and full lines after a chemomechanical polishing. The different spacing of the interference fringes indicates how the polishing decreased the thickness of the sample. Both spectra were measured with light incident from the side of the film. Only a part of the reflectance spectra is shown.

textured layers (σ=24 nm) can be seen. Note, on the other hand, that using the standard theory for the evaluation of the T/R data (it means neglecting the effect of the surface roughness) results in a false, ''apparent'' optical absorption coefficient for textured layers.

A. Study of textured and smooth layers by constant photocurrent method (CPM)

CPM detects the light absorbed (either directly or after one or more scattering events) inbetween the electrodes used for the photocurrent measurement. The gap (spacing) between the electrodes influences the contribution of the scattered light to the measured photocurrent and thus, to the

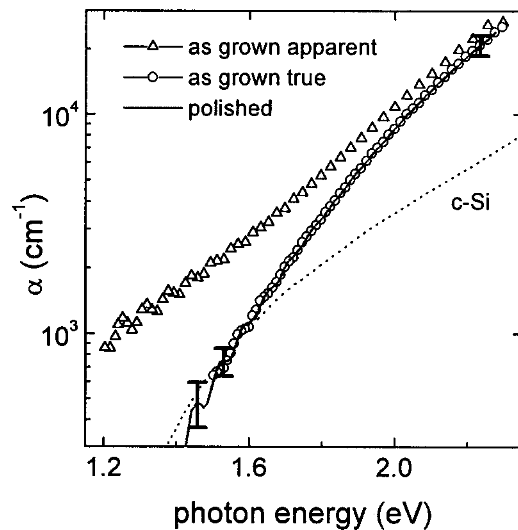

FIG. 4. The apparent absorption coefficient a_{app} (calculated with the assumption σ=0, i.e., by a procedure which does not take into account any surface roughness) and true absorption coefficient α of the film evaluated from the reflectance and transmittance data in Fig. 3. The error bars correspond to the estimated precision of the α evaluation based on the relative error of transmittance measurement (~1%). The absorption coefficient of monocrystalline silicon is shown for comparison.

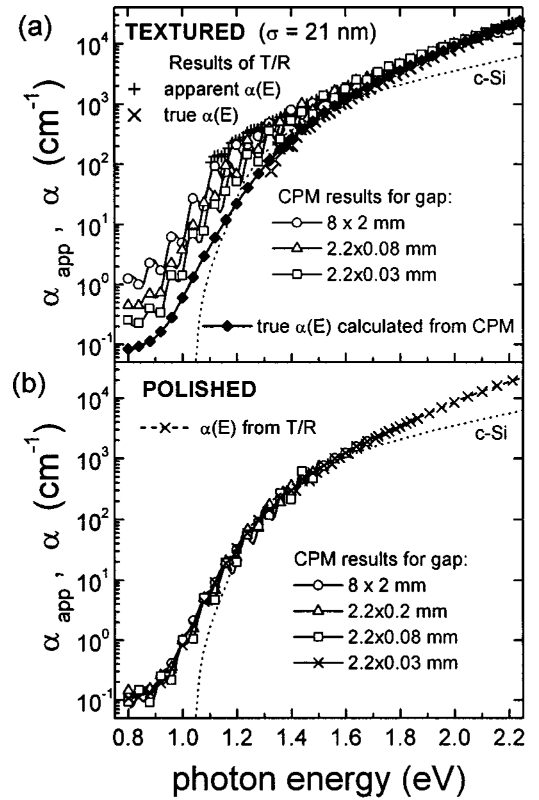

FIG. 5. Apparent optical absorption coefficients of sample A measured by CPM with different interelectrode spacing (gap) and calculated from T/R measurements: (a) in the as-grown state (textured sample) and (b) after a chemomechanical polishing. The evaluated spectral dependence of the true absorption coefficient $\alpha(E)$ is shown as the main result by full diamonds; $\alpha(E)$ of crystalline silicon is shown for comparison. The value of the rms surface roughness of σ=21 nm of the as-grown sample was evaluated from the T/R data.

deduced CPM apparent optical absorption coefficient α_{app} (proportional to the inverse of photon flux necessary to keep the photocurrent constant). CPM results for different interelectrode spacing together with true $\alpha(E)$ determined from T/R measurements and computed from CPM data are shown in Figs. 5 and 6 for the samples with preferential (220) texture. To evaluate our data we have used the theoretical approach described in Sec. II. Figure 5(a) shows the typical sample A with an as-grown (textured) surface and in Fig. 5(b) the same sample with a polished (mirrorlike) surface. We can see that the effect of light scattering on the CPM spectra disappeared with the polishing procedure and CPM measures in this case directly the true $\alpha(E)$.

Figure 6 shows a different class of samples (sample B) again with the as-grown (textured) [Fig. 6(a)] and polished [Fig. 6(b)] surface. For the sample B there is a strong difference in CPM spectra measured with different interelectrode spacing also for the polished surface. This sample was prepared at a high deposition rate (over 1 nm/s) and has a lower mass density, presumably due to voids.

The increase in the deposition rate and the decrease in the defect density (subgap absorption) is an important issue for microcrystalline silicon solar cells. Results presented in Fig. 7 show that it is possible to deposit material with a very low subgap absorption at a deposition rate of around 5 Å/s

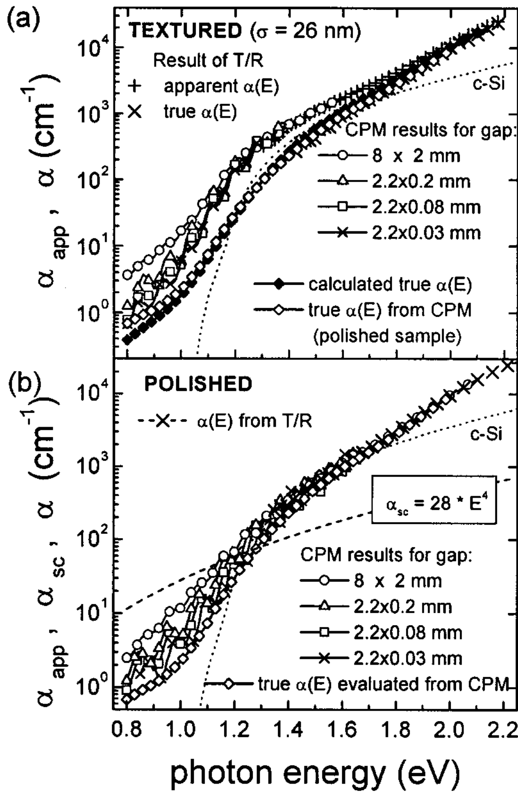

FIG. 6. Apparent optical absorption coefficients of sample B measured by CPM with different interelectrode spacing (gap) and calculated from T/R measurements: (a) in the as-grown state (textured sample) and (b) after a chemomechanical polishing and H_2 plasma treatment. The evaluated spectral dependence of the true absorption coefficient $\alpha(E)$ is shown as the main result by solid or empty diamonds; $\alpha(E)$ of crystalline silicon is shown for comparison. The rms surface roughness $\sigma=26$ nm of the as-grown sample was evaluated from the T/R data.

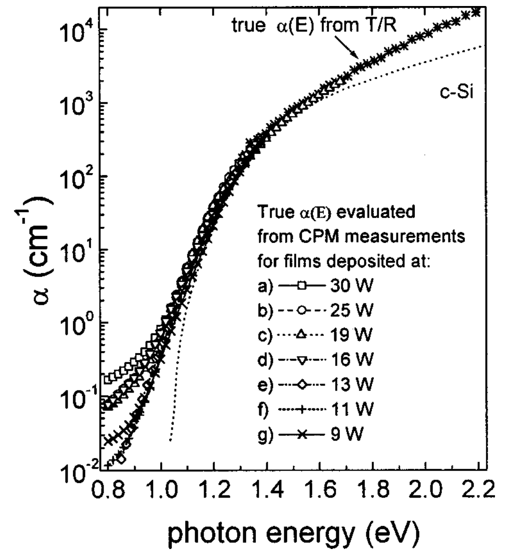

FIG. 7. Comparison of the true optical absorption coefficient a_{true} for a series of μc-Si:H films prepared at different discharge powers and at dilution of silane in hydrogen of 5%.

(for deposition conditions see Ref. 26). These samples [prepared at very high frequency (VHF) power 11 and 13 W] represent the lowest subgap absorption data for microcrystalline silicon presented in the literature so far.

V. DISCUSSION

A. Surface and bulk scattering

The results in Figs. 5(a) and 5(b) for the typical sample A (prepared at a medium growth rate of 6 Å/s) demonstrate the dominant surface scattering to be present in such samples. After a standard chemomechanical polishing of the rough sample surface the scattering disappears and the true optical absorption coefficient α_{true} is directly measured by CPM. On the contrary, sample B (prepared at a higher deposition rate of over 10 Å/s) also exhibits a bulk scattering contribution,[7,12] which cannot be removed by polishing, as it is seen in Fig. 6(b). The evaluated bulk scattering coefficient is $\alpha_{\mathrm{sc}}=28\cdot E^4$, where E is the photon energy (eV). This would point to a hypothesis that small voids are present in microcrystalline silicon prepared at high deposition rates, similarly to the case of amorphous silicon.[12,27] This is furthermore supported by a lower mass density of such films.

It can be useful to unify the theories of bulk and surface scattering, as described in Secs. II C 1 and II C 2, in terms of the scattering coefficient α_{sc}.[28] The case of light scattering at a rough interface, given by the scattering factors S, can be expressed on the basis of the rms surface roughness σ by the scattering coefficient α_{sc}

$$\alpha_{\mathrm{sc}}=\frac{1}{d_f}\left(\frac{2\pi(n_f-n_a)\sigma}{\lambda}\right)^2, \tag{41}$$

where all terms have their usual meaning. Now we can use for the calculation of surface scattering the theory of multiple bulk scattering described in Sec. II C 1.

Surface scattering is of a vital importance for thin film silicon solar cells. Because of indirect optical transitions in crystalline silicon, optical absorption in thin silicon films is rather low and has to be increased in order to absorb most of the solar spectrum in film a few micrometers thick. Therefore, complicated light trapping schemes have been suggested.[29]

An alternative is an ideal ''Lambertian'' light scattering due to a random rough surface.[30] As a special case, we discuss here a random rough surface with rms roughness smaller than the wavelength of the light (nanotextured film). This is exactly the case which has already been realized in a real thin film μc-Si:H cell (2 μm) due to the natural grown surface texture.[3,4,31] The reason for this optical enhancement is presented in a theory here, whereby the s factors are given in Eqs. (3) and (4). In Fig. 8, the square of the scattering factors s is plotted because the reflected or transmitted light intensity is proportional to the square of amplitude. In the case of internal reflection in silicon at the rough silicon/air interface, the rms surface roughness of $\sigma=40$–50 nm removes the specular part of the reflection because $(s_{\mathrm{int}})^2$ approaches zero and one observes just the diffuse reflection (for the wavelength of 900 nm). This is not the case for the transmission through a surface of the same roughness, as it can be seen from Fig. 8. The analysis of this figure (dashed curve for s_{ext}^2) also explains the appearance of the nanotex-

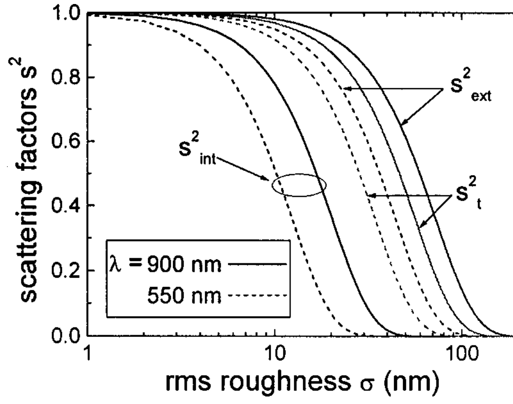

FIG. 8. Reduction of the intensities of light specullary reflected or transmitted at the silicon film–air interface due to light scattering at the rough surface, as a function of the rms surface roughness σ, for wavelengths of 900 nm (full lines) and 550 nm (dashed lines). The reduction is proportional to the square of the scattering factors defined by Eqs. (3) and (4). The index (t) stands for transmitted, the index (ext) for externally reflected and (int) for internally reflected light in Si films.

tured silicon films for the naked eye. A root mean square roughness smaller than 10 nm is difficult to detect by the eyes, a typical roughness 20–30 nm can be easily detected and films with a rms roughness of 200 nm have no specular reflectance (for random, noncorrelated roughness).

All this has a crucial importance for thin film silicon solar cells. Figure 9 shows the Monte Carlo model results of the external quantum efficiency of a thin textured microcrystalline silicon p-i-n solar cell. Details of this modeling will be published elsewhere.[32] The cell consists of a glass superstrate, a front transparent conducting oxide (TCO) layer, 2 μm thin p-i-n μc-Si:H, TCO back contact and a metal back reflector (Ag). All optical material constants and all thicknesses enter in the model, together with the roughness of each interface. In Fig. 9 we assume that all interfaces copy the roughness of the front TCO and that the rms roughness σ varies from 0 to 100 nm. One can observe a pronounced enhancement of the response in the infrared region due to a diffusive light scattering at rough interfaces.

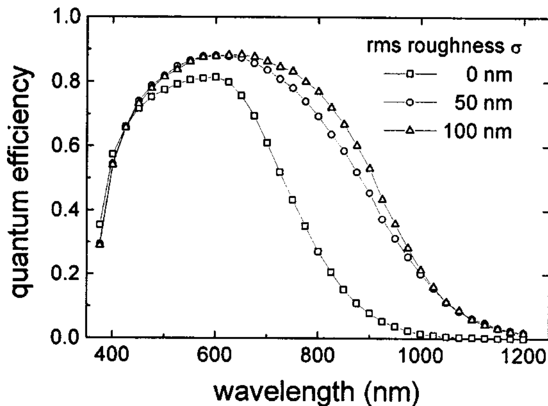

FIG. 9. Calculated spectral dependence of the quantum efficiency for a 2 μm thick microcrystalline solar cell as a function of the interface roughness. The cell consist of the structure: thick glass substrate/ZnO(1 μm)/ p^+(10 nm)/μc-Si:H(2 μm)/n^+(20 nm)/ZnO(1μm)/Ag back reflector. The numbers in brackets indicate the thicknesses of the corresponding layers.

B. Material parameters obtained from the true $\alpha(E)$: Differences between microcrystalline and single crystalline silicon

The spectral dependence of the optical absorption coefficient $\alpha(E)$ of microcrystalline Si gives us the information on the material structure, whereas the subgap part reflects the defect states in the material. In order to compare a standard crystalline silicon material with a typical ''device-quality'' microcrystalline silicon with hydrogen content about 5% (from IR spectra) and 10% amorphous fraction (from Raman scattering) we divide the spectral region into three parts:

(a) the region between 1.2 and 1.4 eV describing the parabolic behavior close to the band edges from which the indirect band gap of silicon may be determined:
(b) the intrinsic absorption region above 1.5 eV; and
(c) the region below 1.1 eV describing the defect-connected absorption.

The detailed study of region (a) on a large set of samples points to the conclusion, that $\alpha_a(E)$ reaches similar values as in the case of crystalline silicon (see Figs. 4–7), hence, the indirect gap of typical device-quality microcrystalline Si has a value of approximately 1.1 eV at room temperature. Small variance between different samples can be related to the internal strain in the layers, as also observed for the case of monocrystalline Si.[33]

The true optical absorption coefficient $\alpha_a(E)$, measured either on nonscattering samples or determined with the help of procedures described in this paper for textured layers, is always higher than the absorption coefficient of crystalline silicon in the above-gap region (b). This enhanced optical absorption brings an important advantage for PV applications. The higher $\alpha(E)$ coefficient can be understood by the effective media approximation[13] taking the combination of three different material components into account: the crystalline silicon grains, the surface region of grains and the amorphous silicon tissue. It is tempting to quantitatively correlate each component with the corresponding part (peak) in Raman specta situated alternatively at 520, 500 and 480 cm^{-1}.

In a single crystalline silicon, the absorption coefficient around 1.1 eV is related to phonon assisted transitions.[25] This mechanism is masked in microcrystalline silicon by an exponential decay (Urbach tail) with a typical slope of 50 meV. The appearance of an exponential decay in μc-Si:H may be interpreted as a result of the loss of translational symmetry at the grain boundaries.

The defect-connected absorption [$\alpha(E)$ below 1 eV] is attributed to silicon dangling bonds mainly at the grain boundaries and in the amorphous tissue.[6,34] This absorption part generally increases with hydrogen evolution at high annealing temperature and decreases with posthydrogenation.[6,34,35] At photon energy of 0.8 eV device-grade microcrystalline silicon shows a typical value of the true optical absorption coefficient below 0.1 cm^{-1}.[7] One can even observe α_{true} values at the photon energy of 0.8 eV as low as 0.01 cm^{-1} (see Fig. 7). A low defect-related absorption is an indication of the high quality of this material. One can observe that at higher applied VHF power, the quality of ma-

terial decreases (increased subgap absorption, reduced solar cell efficiency).[26]

Finally, we want to comment that the evaluation of the optical absorption coefficient of nanotextured microcrystalline silicon films in some previous papers[6,10,34,36] should be reconsidered with the help of theory presented here.

VI. CONCLUSIONS

We have experimentally demonstrated that the absorption enhancement in the infrared region of nanotextured microcrystalline silicon thin films and solar cells comes mainly from the surface scattering. Scattering in the bulk of material can significantly contribute (to the CPM results) in the subgap spectral region. A detailed theory for the evaluation of the true optical absorption coefficient α from transmittance, reflectance and absorptance (CPM) measurements has been presented. Both the scattering at the surface and in the bulk of the film have been taken into account in our theory. The spectral dependence of the absorption coefficient $\alpha(E)$ has been interpreted in terms of defect density, disorder, crystalline and amorphous fractions and material morphology.

ACKNOWLEDGMENTS

This work was supported (Contract No. JOR3-CT97-0145) by the European Commission, project NEST, by Grant Nos. GAAV A1010809, GACR 202/98/0669, and partly by NEDO, Japan and Grant No. GACR 202/99/0403.

APPENDIX A: SCALAR SCATTERING THEORY OF THE REFLECTANCE AND TRANSMITTANCE OF THE LAYER WITH A ROUGH INTERFACE ON A THICK SUBSTRATE

Supposing a light wave is incident perpendicularly to a smooth interface between the media i and j and with complex refractive indexes N_i and N_j. Then the reflection and transmission can be described by the Fresnel coefficients

$$r_{ij}^0=\frac{N_i-N_j}{N_i+N_j}, \tag{A1}$$

$$t_{ij}^0=\frac{2N_i}{N_i+N_j}, \tag{A2}$$

where the superscript 0 corresponds to roughness σ value of zero.

If the interface between media i and j is rough then scattering will lead to a loss of light from the specularly reflected and transmitted beams. The scalar scattering theory[15,28] describes these losses by reducing the Fresnel coefficients by the so called scattering factors. Thus, the coefficients for amplitudes of reflected and transmitted lightwave at a rough interface are given by

$$r_{ij}=r_{ij}^0 s_{ij}^r=\frac{N_i-N_j}{N_i+N_j}\cdot\exp\left[-\frac{1}{2}\left(\frac{4\pi n_i\sigma_{ij}}{\lambda}\right)^2\right], \tag{A3}$$

$$t_{ij}=t_{ij}^0 s_{ij}^t=\frac{2N_i}{N_i+N_j}\cdot\exp\left[-\frac{1}{2}\left(\frac{2\pi(n_i-n_j)\sigma_{ij}}{\lambda}\right)^2\right], \tag{A4}$$

where σ_{ij} is the rms roughness of the interface and λ is the light wavelength in vacuum. The scattering factors s_{ij}^r and s_{ij}^t are equal to unity for smooth surface ($\sigma=0$).

The reflection and transmission coefficients of a thin film on a semi-infinite nonabsorbing substrate can be calculated by the sum of the amplitudes of multiple beams originating from the split incident beam

$$\begin{aligned} r_{123}&=t_{12}e^{-i\delta}r_{23}e^{-i\delta}t_{21}\\ &\quad+t_{12}e^{-i\delta}r_{23}e^{-i\delta}r_{21}e^{-i\delta}r_{23}e^{-i\delta}t_{21}+\dots\\ &=r_{12}+\frac{t_{12}t_{21}r_{23}e^{-2i\delta}}{1-r_{21}r_{23}e^{-2i\delta}}, \end{aligned} \tag{A5}$$

$$\begin{aligned} t_{123}&=t_{21}e^{-i\delta}t_{23}+t_{12}e^{-i\delta}r_{23}r_{21}e^{-2i\delta}t_{23}\\ &\quad+t_{12}e^{-i\delta}r_{23}^2r_{21}^2e^{-4i\delta}t_{23}+\dots\\ &=\frac{t_{12}t_{23}e^{-i\delta}}{1-r_{21}r_{23}e^{-i2\delta}}. \end{aligned} \tag{A6}$$

The subscript 123 indicates that the light is incident from medium 1 on a thin film with index N_2 on the substrate (medium 3) and the phase factor δ can be written as

$$\delta=\frac{2\pi dN_2}{\lambda}. \tag{A7}$$

The phase factor is the sum of two terms $\delta=\varphi/2+i\alpha d/2$, where $\varphi=4\pi n_2 d/\lambda$ describes the interferences (n_2 is the index of refraction) and $\alpha=4\pi k_2/\lambda$ is the extinction coefficient.

We need to convert the amplitude quantities into intensities observed in the experiment. The intensities of the reflected and transmitted beams at an interface between media 1 and 2 (with or without any interfacial layers) are given by

$$R_{12}=r_{12}r_{12}^*, \tag{A8}$$

$$T_{12}=\frac{n_2}{n_1}t_{12}t_{12}^*. \tag{A9}$$

Using the formulas above and substituting the parameters for μc-Si:H (n_f,α,d,σ) and the indices of (nonabsorbing) substrate n_s and ambient n_a one can calculate the reflectance and transmittance of the film on a semi-infinite substrate. Thus one obtains for incidence either from the side of ambient (afs) or substrate (sfa)

$$R_{\rm afs}=\frac{R_{\rm af}+R_{\rm fs}e^{-2\alpha d}+2\sqrt{R_{\rm af}R_{\rm fs}}e^{-\alpha d}\cos(\varphi)}{1+R_{\rm af}R_{\rm fs}e^{-2\alpha d}+2\sqrt{R_{\rm af}R_{\rm fs}}e^{-\alpha d}\cos(\varphi)}, \tag{A10}$$

$$R_{\rm sfa}=\frac{R_{\rm sf}+R_{\rm fa}e^{-2\alpha d}+2\sqrt{R_{\rm sf}R_{\rm fa}}e^{-\alpha d}\cos(\varphi)}{1+R_{\rm sf}R_{\rm fa}e^{-2\alpha d}+2\sqrt{R_{\rm sf}R_{\rm fa}}e^{-\alpha d}\cos(\varphi)}, \tag{A11}$$

$$T_{\rm afs}=T_{\rm sfa}=\frac{T_{\rm af}T_{\rm fs}e^{-\alpha d}}{1+R_{\rm af}R_{\rm fs}e^{-2\alpha d}+2\sqrt{R_{\rm af}R_{\rm fs}}e^{-\alpha d}\cos(\varphi)}. \tag{A12}$$

We still need to include the influence of the substrate back interface in our results. If the substrate is thick enough

(thicker than the coherence length of the monochromatic light used) then the interference effects in the substrate will be suppressed and one has to take the sum of the intensities of the multiple split beams. Thus, in case of incident light from the film side one gets:

$$R_f = R_{\mathrm{afs}} + T_{\mathrm{afs}} R_{\mathrm{sa}} T_{\mathrm{sfa}} + T_{\mathrm{afs}} R_{\mathrm{sa}} R_{\mathrm{sfa}} R_{\mathrm{sa}} T_{\mathrm{sfa}} + \dots$$
$$= R_{\mathrm{afs}} + \frac{T_{\mathrm{afs}} T_{\mathrm{sfa}} R_{\mathrm{sa}}}{1 - R_{\mathrm{sfa}} R_{\mathrm{sa}}}. \tag{A13}$$

In the case of incident light from the glass side

$$R_g = R_{\mathrm{as}} + T_{\mathrm{as}} R_{\mathrm{sfa}} T_{\mathrm{sa}} + T_{\mathrm{as}} R_{\mathrm{sfa}} R_{\mathrm{sa}} R_{\mathrm{sfa}} T_{\mathrm{sa}} + \dots$$
$$= R_{\mathrm{as}} + \frac{T_{\mathrm{as}} T_{\mathrm{sa}} R_{\mathrm{sfa}}}{1 - R_{\mathrm{sfa}} R_{\mathrm{sa}}}. \tag{A14}$$

The transmittance does not depend on the direction of the light beam and is the same for light incident from either the film or glass side of the sample

$$T_f = T_g = T_{\mathrm{afs}} T_{\mathrm{sa}} + T_{\mathrm{afs}} R_{\mathrm{sa}} R_{\mathrm{sfa}} T_{\mathrm{sa}} + \dots = \frac{T_{\mathrm{afs}} T_{\mathrm{sa}}}{1 - R_{\mathrm{sfa}} R_{\mathrm{sa}}}. \tag{A15}$$

APPENDIX B: EFFECT OF MULTIPLE BULK SCATTERING ON THE PHOTOCURRENT MEASUREMENT IN A COPLANAR ELECTRODE CONFIGURATION

The photocurrent I_{sc} arises from the photons absorbed after one or more scattering events. In the case of bulk scattering in the thin film, one can write

$$\begin{aligned} I_{\mathrm{sc}} \approx {} & N_{\mathrm{photons}}[1-\exp(-\alpha_{\mathrm{sc}} \cdot d_f)]\cos\theta[1-\exp(-\alpha_{\mathrm{true}}/\alpha_{\mathrm{sc}})] + N_{\mathrm{photons}}[1-\exp(-\alpha_{\mathrm{sc}} \cdot d_f)] \\ & \times \cos^2\theta \exp(-\alpha_{\mathrm{true}}/\alpha_{\mathrm{sc}})[1-\exp(-\alpha_{\mathrm{true}}/\alpha_{\mathrm{sc}})] + N_{\mathrm{photons}}[1-\exp(-\alpha_{\mathrm{sc}}.d_f)] \\ & \times \cos^3\theta \exp(-2\alpha_{\mathrm{true}}/\alpha_{\mathrm{sc}})[1-\exp(-\alpha_{\mathrm{true}}/\alpha_{\mathrm{sc}})] + N_{\mathrm{photons}}[1-\exp(-\alpha_{\mathrm{sc}} \cdot d_f)] \\ & \times \cos^4\theta \exp(-3\alpha_{\mathrm{true}}/\alpha_{\mathrm{sc}})[1-\exp(-\alpha_{\mathrm{true}}/\alpha_{\mathrm{sc}})] + \dots, \end{aligned} \tag{B1}$$

where N_{photons} represents the number of photons impinging perpendicularly on the sample surface, and θ is the critical angle for total reflection. In this case one can assume that the scattering mean free path (optical length between two scattering events) is $1/\alpha_{\mathrm{sc}}$. Therefore each row of Eq. (B1) represents a contribution to the photocurrent after the next scattering event. The term ''cos θ'' represents the optical losses of the light within two escape cones (given by the refraction indexes of Si and surrounding medium). Here we consider (instead of two angles θ_1 and θ_2 for interfaces air–film and substrate–film) either the higher angle enabling the waveguiding of the scattered light (for the interelectrode spacing below 1 mm) or the effective angle corresponding to the effective index of refraction. The value of this effective refractive index is given not only by the surrounding media but also by the geometry of the gap (area $W \cdot D$) because some part of the light escaping from thin film to glass substrate can return back to the area of electric field

$$\cos\theta = \cos\theta_1 + \cos\theta_2 - \cos\theta_3, \tag{B2}$$

where θ_3 is calculated on the basis of index of refraction of the film n_f, of the substrate n_s, of the substrate thickness d_s and of the interelectrode function $X(W,D)$

$$\theta_3 = \arcsin\left[\frac{n_s}{n_f} \cdot \sin\left(\arctan\frac{X}{2d_s}\right)\right]. \tag{B3}$$

Equation (B1) can be simply rewritten as

$$\begin{aligned} I_{\mathrm{sc}} \approx {} & N_{\mathrm{photons}}[1-\exp(-\alpha_{\mathrm{sc}} \cdot d_f)]\cos\theta \\ & \times [1-\exp(-\alpha_{\mathrm{true}}/\alpha_{\mathrm{sc}})] \cdot \left[1 + \cos\theta \exp\left(-\frac{\alpha_{\mathrm{true}}}{\alpha_{\mathrm{sc}}}\right)\right. \\ & \left. + \cos^2\theta \exp\left(-2\frac{\alpha_{\mathrm{true}}}{\alpha_{\mathrm{sc}}}\right) + \cos^3\theta \exp\left(-3\frac{\alpha_{\mathrm{true}}}{\alpha_{\mathrm{sc}}}\right) + \dots\right]. \end{aligned} \tag{B4}$$

The terms of Eq. (B4) in the brackets form a geometrical series, therefore one can write

$$\begin{aligned} I_{\mathrm{sc}} \approx {} & N_{\mathrm{photons}}[1-\exp(-\alpha_{\mathrm{sc}} \cdot d_f)]\cos\theta \\ & \times \left[1-\exp\left(-\frac{\alpha_{\mathrm{true}}}{\alpha_{\mathrm{sc}}}\right)\right] \frac{\left[\cos\theta \cdot \exp\left(-\frac{\alpha_{\mathrm{true}}}{\alpha_{\mathrm{sc}}}\right)\right]^{N_{\mathrm{bulk}}} - 1}{\cos\theta \cdot \exp\left(-\frac{\alpha_{\mathrm{true}}}{\alpha_{\mathrm{sc}}}\right) - 1}, \end{aligned} \tag{B5}$$

where N_{bulk} is the number of the scattering events inside the region of an electric field between the electrodes (area $W \cdot D$).

APPENDIX C: CALCULATION OF THE INTERELECTRODE SPACING FUNCTION $X(W,D)$

The interelectrode spacing function $X(W,D)$ represents the average distance travelled by the photons after they are scattered in a waveguided direction of propagation before they leave the active area of the electric field between the electrodes. Since the film thickness is much smaller than the dimensions of electrodes (W and D), the determination of the $X(W,D)$ may be solved as a two dimensional problem.

TABLE I. Results of the interelectrode spacing function $X(W,D)$ for the typically used interelectrode distance D and electrode width W (see Fig. 2).

W (mm)	8	8	2.2	2.2	2.2
D (mm)	2	0.5	0.2	0.08	0.03
$X(W,D)$ (mm)	1.695	0.635	0.231	0.115	0.052

For photons originating in a point (w,d) between the electrodes the average distance before loss $x(W,D,w,d)$ is calculated as the average of the distance to the edge of the interelectrode area over the possible directions of the light, i.e., for $\varphi \in <0,2\pi)$. The spacing function $X(W,D)$ is then the average of the $x(W,D,w,d)$ over the whole area between the electrodes, i.e., for w ranging from 0 to W and d from 0 to D

$$X(W,D)=\int_0^W \int_0^D \frac{x(W,D,w,d)}{WD} dwdd. \quad \text{(C1)}$$

Unfortunately, this integral cannot be solved analytically and therefore one has to use a numerical method for the calculation. Examples of the $X(W,D)$ results of typically used gaps $W \cdot D$ are listed in Table 1.

[1] J. Meier, R. Flückiger, H. Keppner, and A. Shah, Appl. Phys. Lett. **65**, 860 (1994).
[2] J. Meier *et al.*, Proceedings of the 13th European PV Conference, Nice 1995, p. 1445.
[3] J. Meier *et al.*, J. Non-Cryst. Solids **227–230**, 1250 (1998).
[4] K. Yamamoto, M. Yoshimi, T. Suzuki, Y. Tawada, Y. Okamoto, and A. Nakajima, Proceedings of the 2nd World Conference on Photovoltaic Energy Conversion, Vienna, July 1998, p. 1284.
[5] K. Saito, M. Sano, K. Matuda, T. Kondo, T. Nishimoto, K. Ogawa, and I. Kajita, Proceedings of the 2nd World Conference on Photovoltaic Energy Conversion, Vienna, July 1998, p. 351.
[6] N. Beck, J. Meier, J. Fric, Z. Remeš, A. Poruba, R. Fluckiger, J. Pohl, A. Shah, and M. Vaněček, J. Non-Cryst. Solids **198–200**, 903 (1996).
[7] M. Vaněček, A. Poruba, Z. Remeš, N. Beck, and M. Nesládek, J. Non-Cryst. Solids **227–230**, 967 (1998).
[8] A. Masuda, R. Iiduka, A. Heya, C. Niikura, and H. Matsumura, J. Non-Cryst. Solids **227–230**, 987 (1998).
[9] F. Diehl, M. Scheib, B. Schröder, and H. Oechsner, J. Non-Cryst. Solids **227–230**, 973 (1998).
[10] S. Vepřek, F.-A. Saarott, and Z. Iqbal, Phys. Rev. B **36**, 3344 (1987).
[11] A. Poruba, Z. Remeš, J. Špringer, M. Vaněček, A. Fejfar, J. Kočka, J. Meier, P. Torres, and A. Shah, Proceedings of the 2nd World Conference on Photovoltaic Energy Conversion, Vienna, July 1998, p. 781.
[12] M. Favre, H. Curtins, and M. Vaněček, J. Non-Cryst. Solids **114**, 405 (1989).
[13] *Handbook of Optics*, 2nd ed., edited by M. Bass (McGraw-Hill, New York, 1995).
[14] A. Shah *et al.*, Mater. Sci. Eng., B **69–70**, 219 (2000).
[15] P. Beckmann and A. Spizzichino, *The Scattering of Electromagnetic Waves from Rough Surfaces* (Pergamon, Oxford, 1963), Chap. 5.
[16] H. C. Van de Hulst, *Light Scattering by Small Particles* (Wiley, New York, 1957).
[17] W. H. Press, S. A. Teukolsky, W. T. Vetterling, and B. P. Flannery, *Numerical Recipes in C* (Cambridge University Press, Cambridge, UK, 1994).
[18] S. G. Tomlin, Brit. J. App. Phys. (J. Phys. D) **1**, 1667 (1968).
[19] M. Vaněček, J. Kočka, A. Poruba, and A. Fejfar, J. Appl. Phys. **78**, 6203 (1995).
[20] M. Vaněček, J. Kočka, J. Stuchlík, Z. Kožíšek, O. Štika, and A. Tříska, Sol. Energy Mater. **8**, 411 (1983).
[21] N. M. Amer and W. B. Jackson, Semicond. Semimet. **21**, 83 (1984).
[22] M. Vaněček, J. Holoubek, and A. Shah, Appl. Phys. Lett. **59**, 2237 (1991).
[23] P. Torres *et al.*, Appl. Phys. Lett. **69**, 1373 (1996).
[24] Z. Yin, H. S. Tan, and F. W. Smith, Diamond Relat. Mater. **5**, 1490 (1996).
[25] M. J. Keevers and M. A. Green, Appl. Phys. Lett. **66**, 174 (1995).
[26] P. Torres, H. Keppner, J. Meier, U. Kroll, N. Beck, and A. Shah, Phys. Status Solidi A **163**, R9 (1997).
[27] D. L. Williamson and A. H. Mahan (private communication).
[28] I. Filinski, Phys. Status Solidi B **49**, 577 (1972).
[29] M. A. Green, *High Efficiency Silicon Solar Cells* (Trans Tech SA, 1987).
[30] E. Yablonovitch and G. D. Cody, IEEE Trans. Electron Devices **ED-29**, 300 (1982).
[31] J. Meier *et al.*, Proceedings of the 2nd World Conference on Photovoltaic Energy Conversion, Vienna, July 1998, p. 375.
[32] J. Špringer and M. Vaněček (unpublished).
[33] M. Saritas and H. D. McKell, J. Appl. Phys. **61**, 4923 (1987).
[34] W. B. Jackson, N. M. Johnson, and D. K. Biegelsen, Appl. Phys. Lett. **43**, 195 (1983).
[35] N. H. Nickel, W. B. Jackson, and N. M. Johnson, Mod. Phys. Lett. B **8**, 1627 (1994).
[36] Z. Iqbal, F.-A. Sarott, and S. Veprek, J. Phys. C **16**, 2005 (1983).